Ecological Indicators 43 (2014) 236–243

Contents lists available at ScienceDirect

Ecological Indicators

journal homepage: www.elsevier.com/locate/ecolind

Fractal approach to estimating changes in soil properties following the establishment of *Caragana korshinskii* shelterbelts in Ningxia, NW China

Guang-Lei Gao [a], Guo-Dong Ding [a,b,*], Yuan-Yuan Zhao [a,b], Bin Wu [a,b], Yu-Qing Zhang [a,b], Shu-Gao Qin [a,b], Yan-Feng Bao [a], Ming-Han Yu [a], Yun-Dong Liu [a]

[a] College of Soil & Water Conservation, Beijing Forestry University, Beijing 100083, PR China
[b] Yanchi Research Station, Yanchi 751500, PR China

ARTICLE INFO

Article history:
Received 9 May 2013
Received in revised form 28 February 2014
Accepted 3 March 2014

Keywords:
Desertification
Vegetation restoration
Soil property
Particle size distribution
Fractal feature

ABSTRACT

To identify the effects of shelterbelt establishment on soil recovery, we compared soil properties at depths of 0–5, 5–10, and 10–20 cm as affected by *Caragana korshinskii* shelterbelts across a chronosequence of soil undergoing restoration for 7, 11, and 26 years, as well as reference grasslands in Ningxia, NW China. Fractal dimension of soil particle size distribution (PSD) was also integrated to describe variations in soil properties. The results indicated that (1) fine particles, total porosity, total nitrogen, phosphorous, and available nitrogen, phosphorous, and potassium increased significantly with plantation age ($p < 0.05$). Sand particles tended to decrease with restoration time, especially in the topsoil layers (0–5 cm). (2) In most cases, selected physicochemical properties of soil in shelterbelts recovered more than in the reference grasslands; moreover, planting *Medicago sativa* had greatly positive effects on soil nitrogen accumulation due to azotification. (3) Fractal dimensions of soil PSD ranged from 2.3946 to 2.6351. Regression analyses showed fractal dimensions had significant linear correlations with soil physicochemical properties ($R^2 = 0.511–0.870$, $p < 0.01$), except total potassium ($R^2 = 0.248$). Therefore, we suggest D as a considerable and reliable parameter to reflect variations in soil properties affecting vegetation restoration efforts, and additionally as an implication of desertification. This improved information will contribute to a better understanding of vegetation solutions for anti-desertification efforts.

1. Introduction

Desertification in China has experienced multiple arid phases throughout the quaternary (Wang et al., 2008). Desertified China includes the vast arid and semiarid northern territory covering an area of more than 1.8 million km^2. Additionally, over the latest centuries, extensive pastoral and agricultural systems have reduced soil fertility and exacerbated land degradation in desertified regions (Zha and Gao, 1997; Chen and Tang, 2005). Generally, desertification is driven by synthesized natural and anthropogenic forces and causes a decrease in the land's ability to produce food and forage, the quantity and quality of fresh water, the land's resilience, and an increase in social costs, poverty, and political instability (Chen and Duan, 2009). As a consequence, desertification has been widely recognized as a major environmental and social problem and one of the most serious threats to the survival and development of humanity (Wang et al., 2008). Furthermore, easterly winds sweep particulate matter in arid and semiarid China to Japan, Korea, and sometimes to the US (Normile, 2007). Therefore, desertification in China has not only been a regional environmental problem, but a global issue relating to environment and public health (Otani et al., 2012).

The world has reached a broad consensus that appropriate vegetation restoration is the most beneficial, efficient, and sustainable solution for degraded land rehabilitation and combating desertification (Tavili and Jafari, 2009). Since the late 1990s, China has been implementing unprecedented greening efforts to combat desertification including the Six Key Forestry Programs (Li, 2004). At present, China has the world's largest forest plantations, accounting for approximately 62 million hectares. It is widely recognized

* Corresponding author at: College of Soil & Water Conservation, Beijing Forestry University, No. 35 Qinghua East Road, Haidian District, 100083 Beijing, PR China. Tel.: +86 10 6233 6624; fax: +86 10 62338255.
E-mail addresses: gaoguanglei@bjfu.edu.cn (G.-L. Gao), dingguodong@bjfu.edu.cn (G.-D. Ding), yuanyuan0402@126.com (Y.-Y. Zhao), wubin@bjfu.edu.cn (B. Wu), zhangyq@bjfu.edu.cn (Y.-Q. Zhang), qinshugao204@163.com (S.-G. Qin), baoyanfeng2005@126.com (Y.-F. Bao), 490705356@qq.com (M.-H. Yu), u0sniper@qq.com (Y.-D. Liu).

http://dx.doi.org/10.1016/j.ecolind.2014.03.001
1470-160X/

that vegetation restoration has positive effects on soil recovery. Moreover, soil response to vegetation restoration across diverse arid and semiarid regions has been widely studied in China (Duan et al., 2004; Li et al., 2004, 2007; Su et al., 2005; Jiao et al., 2011). For example, vegetation restoration in the Tengger Desert resulted in positive effects on soil water availability, clay and silt contents, as well as nutrients (Duan et al., 2004; Li et al., 2004, 2007). However, although many Chinese researchers and government officials have declared that reforestation has successfully controlled desertification and dust storms, there is surprisingly little unassailable evidence to support their claims (Wang et al., 2010). Scholars' skepticism of Chinese greening efforts seems to be overstated; some even claim that excessive reliance on afforestation in China's arid and semiarid regions has failed to solve the desertification problem (Cao, 2008; Cao et al., 2011). Additionally, arid and semiarid China has large variability due to the differences in climate, soils, and vegetation (Wang et al., 2008). Therefore, more studies are urgently needed to provide basic information that investigate greening program efforts and support a more scientific, effective, and flexible environmental restoration policy.

Yanchi County is located in the Ningxia Hui Autonomous Region in the central part of southern rim area of the Mu Us Desert. Before the 1990s, the total area of desertified land in Yanchi County had increased sharply and reached a peak value in 1989 of 2366.7 km^2 (Chen and Duan, 2009). However, due to logging and grazing control and vegetation restoration efforts, this desertification in Yanchi has begun to diminish by the 1990s (Qi et al., 2003). In this paper, we hypothesized that local soil properties are largely a consequence of plant growth during secondary succession. The physical and chemical properties of the soil as affected by *Caragana korshinskii* shelterbelts across a chronosequence of soil undergoing restoration for 7, 11, and 26 years, as well as reference grasslands were investigated, and the changes in soil bulk density, total porosity, and particle size distribution (PSD), as well as soil organic carbon (SOC) and nutrient contents were analyzed. As an integrated surrogate, fractal dimension of soil PSD were determined to represent the variations in soil properties and desertification. Additionally, in this paper, the focus is primarily at the smaller site scale rather than at the landscape scale.

The objectives of this study are: (1) to identify the effects of shelterbelt establishment on soil physical and chemical properties over time during vegetation restoration; (2) to demonstrate how the soil physicochemical attributes add to fractal features and the potential possibility of fractal dimension as an indicator to imply desertification. This study will provide basic information for our better understanding of anti-desertifications solutions and a firm basis for future policy-making on how best to combat desertification.

2. Materials and methods

2.1. Description of study area

The study sites are located at Yanchi County of Ningxia Hui Autonomous Region, NW China (37°04′–38°10′ N, 106°30′–107°47′ E, at 1400–1800 m above mean sea level) (Fig. 1). This is a typical transitional zone where the terrain changes from the Loess Plateau (South) to the Ordos Plateau (North) (Chen and Duan, 2009). The climate in the study area is a warm temperate monsoon climate. The mean daily temperature is 7.8 °C with an annual winter–summer and diurnal–nocturnal differences of 28 and 20 °C, respectively. The mean annual precipitation is 292 mm and about 62% of this falls between July and September. The mean annual evaporation is 2024 mm, which is dramatically higher than annual precipitation (Gao et al., 2014). The study area is characterized by large dense sand dunes and a hard ridge region covered by sands; the perennially NW winds with a mean annual velocity of 2.6 m/s cause frequent and strong wind erosion (Bao et al., 2013). The aeolian soil is loose, infertile and mobile, and can be classified as arenosols of quartisamment (U.S. Soil Taxonomy) commonly found in arid and semiarid regions. The predominant native plants are *C. korshinskii*, *Hedysarum scoparium*, *Artemisia ordosica*, and *Sophora alopecuroides*.

The field sampling units are located in an enclosed area within Xiawangzhuang Village in Yanchi County on the southern edge of the Mu Us Desert. The adjacent experimental sites never exceeded 5 km in the flat hard ridge region covered by aeolian sands. In the sampling area, arable lands under traditional agricultural systems were converted to grasslands for desertification control purposes. *C. korshinskii* shelterbelts were established using the same methods in 1986, 2001, and 2005, respectively. To achieve more efficient land utilization and greater fertility improvement, *Medicago sativa* were interplanted between the belts, and were reaped annually.

2.2. Study approach and experimental design

As there were no historical data recording changes in most soil properties since the shelterbelts's establishment, we used a classical "space for time" substitution, sampling sites of differing ages (Li et al., 2007). Furthermore, soil from 0 to 20 cm depth was the focus because of the important influence on soil properties by vegetation restoration of the surface soil layer (Jiao et al., 2011). Field research was conducted in August, 2012. For each shelterbelt site (Sites 1–3), three soil sampling profiles were selected at random on the artificial grasslands between the windbreaks. The intact and mixed soil samples were collected at 3 different depths: 0–5, 5–10, and 10–20 cm. A classical survey was used to investigate vegetation characteristics. In each site, three 50 m line transects were selected, and five 1 m × 1 m subplots were evenly distributed for investigation. Meanwhile, adjacent natural grasslands were selected for sampling as well for reference purpose (Sites 4–6). Among them, we found Site 4 with signs of grazing. General information from the sites is described in Table 1.

Soil bulk density and porosity were measured using intact soil cores from each soil layer with three replicates (oven-dried at 105 °C). Soil bulk density was calculated using Eq. (1). Total porosity was subsequently calculated with Eq. (2) using soil bulk density data (Huang, 2010):

$$B_d = (M_s - M_c)/V \quad (1)$$

where B_d is the soil bulk density (g cm^{-3}); M_s is the weight of intact soil core after drying (g); M_c is the weight of soil core sampler (g); and V is the volume of soil core (cm^3):

$$P_t = W_m B_d \quad (2)$$

where P_t is the total soil porosity (%); W_m is the soil's maximum moisture content (g cm^{-3}).

All soil samples were air-dried and passed through 2 and 0.25 mm sieves prior to laboratory analysis. International standard methods adopted and published by the Institute of Soil Science, Chinese Academy of Sciences (1978) were used to analyze soil samples. Soil organic carbon (SOC) was measured by the potassium dichromate wet combustion method. Total nitrogen (N_T) was measured using the micro-Kjeldahl's method. Total phosphorus (P_T) was measured using the Mo–Sb colorimetry method. Total potassium (K_T) was measured using the hydrofluoric and perchloric acid (HF–HCLO acid)-flame photometer method. Available nitrogen (N_{Avi}) was measured using the alkali diffusion method. Available phosphorus (P_{Avi}) was measured by sodium bicarbonate ($NaHCO_3$) digestion–Mo–Sb colorimetry method. Rapid available potassium

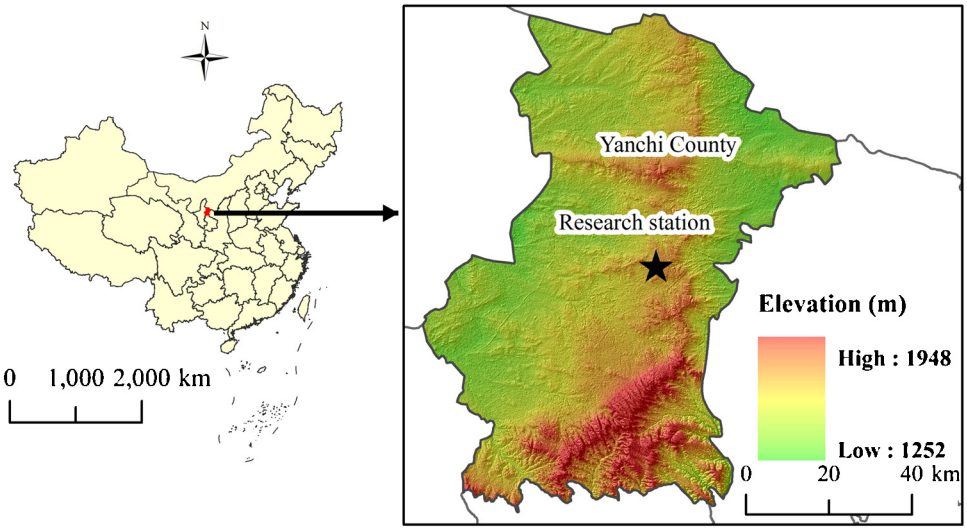

Fig. 1. Location of the study area.

Table 1
General information of the different shelterbelt sites.

Site	Land use	Vegetation type	Restoration years	Coverage (%)
1	Shelterbelt	*Medicago sativa, Pennisetum centrasiaticum*	26	68
2	Shelterbelt	*M. sativa, Artemisia blepharolepis*	11	71
3	Shelterbelt	*M. sativa, A. blepharolepis*	7	52
4	Grassland	*P. centrasiaticum, Agropyron mongolicum*	–	45
5	Grassland	*Cyperus rotundus, Artemisia scoparia*	–	58
6	Grassland	*Agropyron cristatum, A. scoparia*	–	68

(K_{Avi}) was measured using the ammonium acetate digestion-flame photometer method.

To measure the soil particles and fractal characteristics, soil samples were pretreated in an H_2O_2 solution (30%, w/w) to destroy the organic matter. And then, the soil aggregates were dispersed by adding sodium hexametaphosphate (NaHMP) and sonicating the samples for 30 s (Wang et al., 2006; Gui et al., 2010). Furthermore, the pretreated soil samples were analyzed using a laser diffraction technique by Malvern MS 2000 (Malvern, England) with measurement range and error of 0.02–2000 μm and <2%, respectively. Each sample was measured 5 times for arithmetic mean value. The analysis results of soil PSD were output by US Soil Taxonomy standards as follow: clay (0–2 μm), silt (2–50 μm), and sand (50–100, 100–250, 250–500, 500–1000, and 1000–2000 μm).

Coupling models are commonly used for evaluating soil responses to environmental changes (Basso et al., 2012). In this study, the fractal dimension of soil PSD was calculated based on the volume distribution of soil particle size (Wang et al., 2005; Gui et al., 2010). The equation is expressed as:

$$\frac{V(r < R_i)}{V_T} = \left(\frac{R_i}{R_{max}}\right)^{3-D} \quad (3)$$

where r is the soil particle size, R_i is the soil particle size of grade i, R_{max} is the mean diameter of the largest particle grade, $V(r < R_i)$ is the volume of soil particle sizes less than R_i, V_T is the volume of all of soil particles, and D is the volume-based fractal dimension.

2.3. Data analysis

Soil property comparisons among the different sites were restricted by depth. One-way analysis of variance (ANOVA) was conducted using SPSS software (Version 17.0). The LSD test (at $p < 0.05$) was used to compare the means of soil variables. The results of ANOVA were significant at the level of $p < 0.05$. The Pearson correlation coefficient was used to evaluate relationships between D and the selected soil properties. The 2-tailed test was used to distinguish the significant difference of the correlation ($p < 0.01$).

3. Results

3.1. Soil physical structure

Physical analyses of the soil revealed the changes in soil PSD, bulk density, and total porosity in the selected sites (Tables 2 and 3). The clay, silt, and sand particle contents differed significantly. Among them, the mean clay and silt contents for each site increased 0.07–4.28% and 7.45–30.06% during the period after the establishment of *C. korshinskii* shelterbelts, in addition to the decrease in sand particle contents by 7.52–34.35%, respectively. Furthermore, in most cases, the *C. korshinskii* shelterbelt sites had greater clay and silt contents (4.32% and 42.38%), but lower sand contents (53.30%) as compared to the matched grasslands. Accompanying the variations in soil PSD, soil bulk density and total porosity changed as well (Table 3). Soil bulk density decreased more with the increase in restoration age, but was lower than that of the matched grassland. Meanwhile, soil bulk density within the same site increased by 0.05–0.12 g cm^{-3} with increasing soil depth. In contrast, total porosity showed a reverse trend to bulk density; total porosity increased with restoration time and was higher than the matched grassland. Moreover, the surface layer had greater total porosity. It is clear that the establishment of *C. korshinskii* shelterbelts has had an important influence on the investigated soil's physical structure, especially of the surface soil layer (0–5 cm).

Table 2
Variations of soil PSDs for the different shelterbelt sites.

Site	Layer (cm)	Soil PSD (%)		
		Clay (0–2 μm)	Silt (2–50 μm)	Sand (50–2000 μm)
1	0–5	6.58 (1.49)a	62.41 (10.87)a	31.01 (12.35)a
	5–10	6.50 (1.66)a	45.37 (17.19)a	48.13 (18.84)a
	10–20	6.27 (0.58)a	38.30 (19.68)ab	55.43 (19.82)a
2	0–5	4.08 (0.03)b	30.94 (2.92)bc	64.99 (2.89)b
	5–10	3.05 (0.20)b	29.23 (3.30)bc	67.72 (3.50)bc
	10–20	2.89 (0.06)bc	31.49 (3.36)ab	65.62 (3.39)ab
3	0–5	3.34 (0.19)bc	50.06 (4.17)d	46.60 (4.36)c
	5–10	3.10 (0.08)b	49.68 (4.11)a	47.72 (4.19)a
	10–20	3.07 (0.16)bc	43.96 (5.46)a	52.97 (5.58)a
4	0–5	1.57 (0.29)d	15.38 (3.86)e	83.06 (3.62)d
	5–10	2.28 (0.36)b	15.61 (2.65)c	82.11 (2.85)c
	10–20	2.66 (0.36)c	24.90 (4.01)b	72.45 (4.33)b
5	0–5	2.61 (0.39)cd	28.43 (0.98)b	68.96 (1.05)b
	5–10	3.27 (0.09)b	30.68 (2.67)b	66.05 (2.63)b
	10–20	3.35 (0.24)b	34.00 (7.72)ab	62.64 (7.95)ab
6	0–5	3.15(0.29)bc	39.41(7.70)cd	57.44(7.89)bc
	5–10	3.15(0.32)b	38.60(7.68)ab	58.25(7.72)ab
	10–20	3.01(0.40)bc	43.33(4.63)a	53.66(4.41)a

Values in the parentheses indicate standard error ($n = 3$). Different letter in the same column of same layer are significantly different at the 0.05 level (LSD).

Table 3
Variations of bulk density and total porosity for the different shelterbelt sites.

Item	Layer (cm)	1	2	3	4	5	6
Bulk density($g\,cm^{-3}$)	0–5	1.24 (0.07)a	1.35 (0.04)ab	1.39 (0.04)b	1.46 (0.03)b	1.47 (0.05)b	1.41 (0.05)b
	5–10	1.31 (0.06)a	1.37 (0.10)ab	1.40 (0.04)ab	1.55 (0.07)c	1.48 (0.06)bc	1.44 (0.00)bc
	10–20	1.36 (0.06)a	1.40 (0.08)ab	1.46 (0.06)ab	1.58 (0.03)c	1.49 (0.04)bc	1.47 (0.03)abc
Total porosity (%)	0–5	52.64 (7.01)a	46.53 (0.40)b	46.01 (2.25)b	36.55 (3.13)c	43.36 (1.75)b	45.56 (1.56)b
	5–10	49.34 (6.20)a	45.12 (3.99)ab	45.50 (1.71)ab	40.12 (0.52)b	43.11 (1.69)b	45.07 (3.46)ab
	10–20	49.22 (5.97)a	46.35 (4.94)a	44.61 (2.32)ab	39.00 (1.02)b	43.88 (4.99)ab	43.86 (2.77)ab

Values in the parentheses indicate standard error ($n = 3$). Different letter in the same row are significantly different at the 0.05 level (LSD).

3.2. Soil chemical properties

As we can be seen in Table 4, the improvement of soil's physical structure was accompanied by the significant accumulation of SOC and nutrients. The shelterbelt made soil prosper with restoration time; the oldest shelterbelt site had the most fertile soil. Furthermore, in most cases, SOC and nutrients at each depth were several times higher in the shelterbelt sites than compared to the grasslands; statistical analysis showed that this is obvious in the shelterbelt sites built in 1986. For instance, the increases in SOC were 2.4, 2.2, and 1.4 times higher for each soil depth, respectively, after the establishment of *C. korshinskii* shelterbelts in 1986, as compared to the matched grasslands. Furthermore, soil nitrogen accumulation was faster than other nutrients. In the shelterbelts site established in 1986, N_T and N_{Avi} were 4.9, 4.3, 3.7 and 2.8, 2.0, 2.1 times higher than the adjacent grasslands. Additionally, soil nutrients recovered less with an increase in soil depth; however, soil K_T presented an exception. Soil K_T decreased in for each soil depth with time in restoration areas. Moreover, Soil K_T contents in the sites with shelterbelts were even lower than the adjacent grasslands.

3.3. Soil fractal characteristic and the relationships with soil properties

As shown in Table 5, fractal dimensions were calculated by soil PSD data using Eq. (3). Overall, the fractal dimensions for different sites varied from 2.3946 to 2.6351; *D* values in site (1) and (4) differed significantly from other sites. The mean fractal dimensions in the shelterbelt sites (2.5582 ± 0.0501) were much higher than the mean *D* values in the adjacent grasslands (2.4918 ± 0.0452). Mean *D* values of the shelterbelt sites and grassland sites differed from each other as depth increased. Generally, the mean fractal dimensions decreased successively with the increasing soil depth in shelterbelt sites; in contrast, the surface (0–5 cm) had the lowest mean fractal dimensions value in the matched grasslands sites.

Linear regression analyses were performed to identify the strength of correlations between fractal dimensions of soil PSD and selected soil properties (Figs. 2 and 3). Relating to soil physical properties (Fig. 3), the fractal dimensions had strong positive correlations with clay ($R^2 = 0.870$), silt contents ($R^2 = 0.598$), and total porosity ($R^2 = 0.654$). Conversely, we found negative correlations with the content of sand particles ($R^2 = 0.667$), and bulk density ($R^2 = 0.511$). Relating to soil chemical properties, the *D* values had positive correlations with SOC, N_T, P_T, N_{Avi}, P_{Avi}, and K_{Avi} ($R^2 = 0.555$–0.707, Fig. 3a–c and e–g), and a weak negative correlation with K_T ($R^2 = 0.248$, Fig. 3d). Overall, no matter the soil physical or chemical properties, regression analysis showed that an increase in the fractal dimensions of soil PSD implies the soil physical structure improvement and fertility recovery.

4. Discussion

4.1. Changes in soil properties after C. korshinskii shelterbelts establishment

In desertified Northern China, wind erosion can be reversed through the implementation of vegetation restoration solutions, including afforestation, aerial seeding, and straw checkerboards (Li et al., 1999, 2006; Su et al., 2005). These measures provide

Table 4
Variations of soil organic carbon and nutrients for the different shelterbelt sites.

Site	Layer (cm)	SOC (g kg^{-1})	N_T (g kg^{-1})	P_T (g kg^{-1})	K_T (g kg^{-1})	N_{Avi} (mg kg^{-1})	P_{Avi} (mg kg^{-1})	K_{Avi} (mg kg^{-1})
1	0–5	8.55 (0.53)a	0.50 (0.05)a	1.43 (0.13)a	16.58 (1.57)ab	36.43 (1.12)a	4.99 (0.57)a	173.83 (10.54)a
	5–10	7.93 (0.52)a	0.47 (0.06)a	1.27 (0.18)a	13.83 (1.11)a	29.81 (0.32)a	4.13 (0.31)a	135.83 (22.54)a
	10–20	6.95 (0.99)a	0.42 (0.02)a	1.36 (0.01)a	13.90 (1.66)a	33.63 (6.18)a	3.72 (0.26)a	122.33 (10.37)a
2	0–5	7.15 (0.40)b	0.36 (0.03)b	1.32 (0.02)ab	15.09 (0.23)a	30.54 (2.74)ab	3.38 (0.30)b	122.50 (17.69)b
	5–10	5.83 (0.26)b	0.33 (0.00)b	1.28 (0.07)a	15.16 (0.25)ab	29.03 (3.71)a	1.62 (0.35)b	103.17 (5.86)b
	10–20	5.83 (0.28)ab	0.24 (0.02)b	1.28 (0.05)a	15.44 (1.13)ab	22.87 (3.04)b	2.12 (0.20)b	82.83 (5.69)b
3	0–5	6.16 (0.49)bc	0.31 (0.05)bc	1.15 (0.11)b	14.41 (2.99)a	26.70 (4.02)bc	1.80 (0.24)c	102.50 (21.52)bc
	5–10	5.24 (0.08)b	0.24 (0.04)c	1.16 (0.17)a	17.59 (2.29)bc	21.03 (4.66)b	1.70 (0.49)b	94.33 (4.16)b
	10–20	4.40 (0.50)c	0.23 (0.03)b	1.17 (0.17)ab	18.85 (1.98)bc	18.78 (6.43)b	1.34 (0.30)c	91.00 (9.04)b
4	0–5	3.62 (0.78)d	0.10 (0.02)d	0.76 (0.06)c	18.46 (1.11)bc	12.97 (3.93)d	1.07 (0.07)d	59.50 (4.36)e
	5–10	3.58 (0.79)c	0.11 (0.01)d	0.91 (0.05)b	19.22 (0.75)cd	15.24 (2.28)c	0.89 (0.18)c	56.67 (3.88)c
	10–20	4.99 (0.72)bc	0.11 (0.03)c	0.95 (0.20)b	20.32 (1.98)c	16.11 (2.44)b	0.65 (0.05)d	55.00 (4.77)d
5	0–5	6.17 (0.49)bc	0.29 (0.03)c	1.21 (0.08)b	19.95 (1.43)c	20.91 (2.66)c	2.00 (0.08)c	84.33 (10.77)cd
	5–10	5.63 (0.47)b	0.25 (0.03)c	1.13 (0.02)ab	20.02 (1.67)d	13.57 (2.07)c	1.61 (0.18)b	71.33 (12.85)c
	10–20	5.67 (0.98)b	0.22 (0.01)b	1.13 (0.02)ab	17.90 (3.19)bc	19.65 (6.00)b	1.42 (0.16)c	66.17 (1.04)cd
6	0–5	5.90 (0.63)c	0.28 (0.02)c	1.23 (0.15)b	17.31 (1.13)abc	22.55 (3.86)c	1.75 (0.37)c	69.83 (5.58)de
	5–10	5.49 (0.28)b	0.26 (0.00)c	1.13 (0.13)ab	17.71 (1.12)cd	20.41 (0.76)b	1.32 (0.05)bc	70.17 (2.75)c
	10–20	5.30 (0.29)bc	0.24 (0.03)b	1.14 (0.17)ab	18.43 (1.27)bc	20.66 (2.43)b	1.20 (0.06)c	68.83 (1.53)c

Values in the parentheses indicate standard error ($n = 3$). Different letter in the same column of same layer are significantly different at the 0.05 level (LSD).

Table 5
Variations of fractal dimensions of soil PSD for the different shelterbelt sites.

Layer (cm)	1	2	3	4	5	6
0–5	2.6351 (0.0363)a	2.5484 (0.0027)b	2.5408 (0.0109b	2.3946 (0.0163)c	2.4869 (0.0203)d	2.5246 (0.0166)b
5–10	2.6199 (0.0460)a	2.5083 (0.0130)b	2.5310 (0.0067)b	2.4472 (0.0231)c	2.5201 (0.0037)b	2.5227 (0.0157)b
10–20	2.6106 (0.0238)a	2.5041 (0.0060)bc	2.5259 (0.0099)b	2.4830 (0.0219)c	2.5258 (0.0178)b	2.5210 (0.0166)b

Values in the parentheses indicate standard error ($n = 3$). Different letter in the same row are significantly different at the 0.05 level (LSD).

crucial protections against strong and perennial winds that lead to soil erosion. In this paper, using a substitution of "space for time", our study reveals that the establishment and development of the *C. korshinskii* shelterbelt on eroded soil causes significantly positive changes in physical and chemical properties of soil. During this restoration process, fine particles lower than 50 μm (clay and silt) significantly increased, whereas sand fractions greatly decreased, indicating that the reversal of desertification by vegetation accompanied progressively accumulation of fine-particle soil. Moreover, we found that SOC and soil nutrients tended to increase with the accumulation of clay and silt particles. Conclusively, wind-induced desertification not only causes the transportation of soil particles, but accompanies soil carbon, nutrient, and functional losses. Similar conclusions have been reached suggesting that SOC and nutrient content are closely associated with fine particles soil rather than coarse sand, throughout the world (Carter et al., 2003; Rumpel et al., 2004; Arrouays et al., 2006; Jin et al., 2013).

The shelterbelts have more efficient water use efficiency than other vegetation solutions for anti-desertification, but greatly diminish wind's effects by increasing aerodynamic roughness lengths (Yang et al., 2006). As a consequence, a higher threshold wind velocity is helpful to protect vulnerable fine surface soils. Meanwhile, the shelterbelts capture soil particles while obstructing airflow. Furthermore, the shelterbelts provide a relatively stable

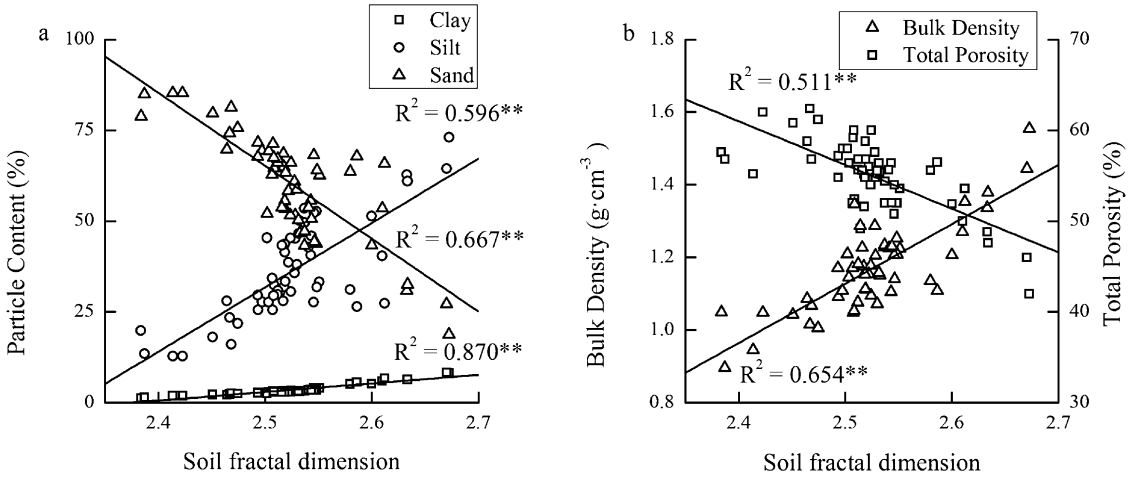

Fig. 2. Relationships between *D* values and soil physical properties: (a) particle content and (b) bulk density and total porosity. **Correlation is significant at the 0.01 level (2-tailed).

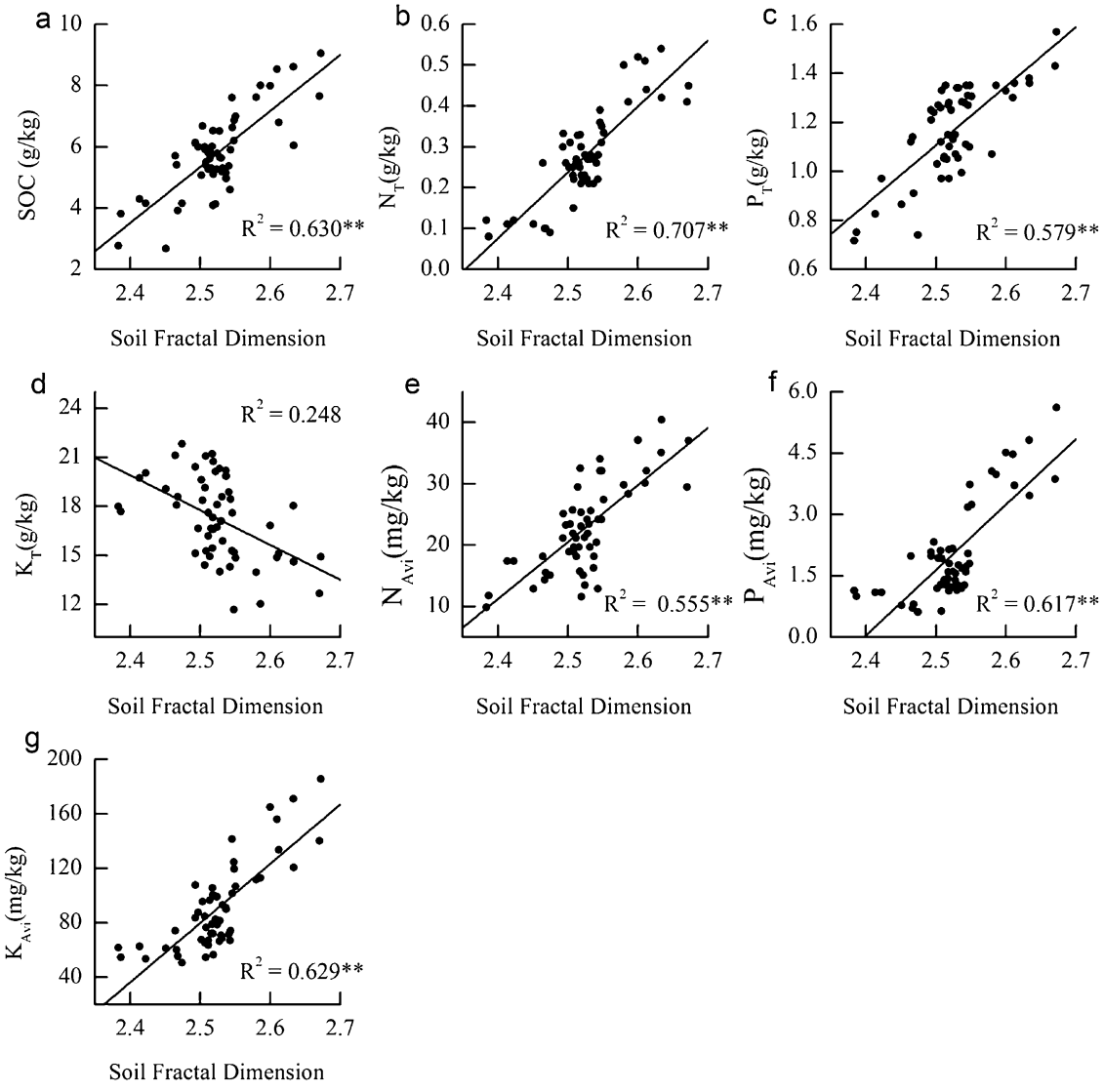

Fig. 3. Relationships between *D* values and SOC and nutrients: (a) SOC, (b) N_T, (c) P_T, (d) K_T, (e) N_{Avi}, (f) P_{Avi}, and (g) K_{Avi}. **Correlation is significant at the 0.01 level (2-tailed).

microclimate and microenvironment. Compared to the bare grasslands, the shelterbelts areas have weaker erosive winds, lower illumination, and lower evaporation. Therefore, xerophytic plants are better at invading and succeeding to in survival and development.

Species selection is one of the key factors of great importance for environmental restoration in arid and semiarid regions. China is a vast country with a diverse physical environment that provides unusually favorable conditions for the survival and development of a large number of plant species (Li, 2004). There are numerous plants used to combat desertification. However, among them, some succeed while others fail (Yang, 1996). Improper species selection will lead to plants not adapting to the hostile environment of drought, leading to failure of restoration (Cao, 2008). In our study, the shelterbelts were formed by native *C. korshinskii*, well known for its ability to resist drought in northwest China (Xu et al., 2012). The sparse shelterbelts in banding collocate can provide the basic requirements for water and nutrients. Meanwhile, the planting *M. sativa* is also a native species and commonly cultivated as high quality forage grass. Furthermore, as leguminous plants, rhizobias of *C. korshinskii* and *M. sativa* help the nitrogen-poor soils prosper due to the azotification.

4.2. Fractal approach to estimate variations in soil properties and the implication for desertification

In arid and semiarid regions, soil PSD determines the movement of solutes, heat, and air (Su et al., 2004). More importantly, soil PSD affects the amount, position, and time of water infiltration into desert soil, and the water distribution in a soil profile (Tyler and Wheatcraft, 1990). Therefore, soil PSD is a commonly used surrogate to reflect soil environment change induced by desertification (Jin et al., 2013). Previously, soil quality was thoroughly investigated by individual fractions and textual analysis characterizing soil PSD. However, individual fractions emphasize nutrient-rich fine particles (Gao et al., 2014), and textual analysis usually fails to represent the differentiations of the same or similar soil types. Therefore, these methods are faulty in investigating real soil systems, especially regarding the coarse aeolian soil in arid and semi-arid regions. In the past few decades, a fractal approach has been integrated into soil science. Modeling all soil PSD information, fractal dimensions are proven to be well matched with various soil properties and exhibits only slight differences in independent soil system studies (Wang et al., 2006; Gui et al., 2010; Jin et al., 2013). Therefore, fractal methodology is of considerable

intrinsic interest; fractal dimensions of soil PSD can be used as a practical and descriptive index for quantifying soil degradation (Falconer, 2003). Our analysis also supports this correlation.

Fractal dimensions of soil PSD directly estimate variations in soil properties and can imply desertification. In the desertification process, wind-induced selective removal of fine particle size soil is accompanied by physical structure damages, organic matter and nutrient loss, water-holding capacity decrease, as well as some biological property depletion of soil (Su et al., 2004). During the reversal of desertification, due to the protection and fertilization of xerophytic plants and artificial engineering (e.g. the straw checkerboard technique), soil clay and silt particles increase and sand particles decrease accompanying SOC and soil nutrient recovery and improvement. In short, the decrease of D values indicates soil particle coarsening and soil nutrient loss, and the increase of D values indicates the soil particles refinement mentioned above. Fractal dimensions are not only a sensitive parameter to reflect variations in soil properties, but a considerable and reliable surrogate relating to the desertification process.

In practice, the fractal approach realizes the possibility of quantifying estimations of the variations in soil properties by using a single parameter. China has been implementing unprecedented large scale environmental restoration efforts to combat desertification in arid and semiarid regions. Fractal dimensions provide an efficient and useful tool for the assessment of program's efficacy. Moreover, fractal dimensions also signal a potential risk of wind-induced erosion. Generally, areas with high D values indicate abundant fine particles and fertilizer. However, once land loses its precious xerophytic plants as a protector, the loose soil will endure strong dry-hot wind. Fertile soil will be eroded in a short term, while gaining it back is a long-term process. According to our study, light grazing caused significant soil erosion induced by wind. Scientific conservation and management of existing natural and artificial vegetations, as well as the engineering measures, is as important or more important than the on-going works.

5. Conclusions

C. korshinskii shelterbelts represent an important vegetation restoration type to combat desertification and are widely used in arid and semiarid regions of desertified Northern China. According to our study, after the establishment of *C. korshinskii* shelterbelts, positive changes in most of the selected soil physical and chemical properties within the shelterbelts were more rapid than in adjacent, untreated grasslands. Furthermore, we believe that the planting of *M. sativa* has greatly improved soil nitrogen due to azotification. Fractal analysis showed that there existed significant ($p < 0.05$) linear relationships between PSD-based fractal dimensions and measured soil properties. Thus, we recommended D as a sensitive and considerable integrated surrogate to reflect and assess variations in soil properties implying desertification. This study provides basic information on desertification processes and is instructive on desert ecosystem restoration.

Acknowledgements

We gratefully thank Prof. Hai-Yan Wang (Beijing Forestry University) and Jon Gartner for their generous help in writing this manuscript as well as the great cooperation with the Environmental Protection and Forestry Bureau of Yanchi County, Ningxia Hui Autonomous Region. This work was funded by one of National Basic Research Program of China (2013CB429906) and the National Technology & Science Support Program of China (2012BAD16B02).

References

Arrouays, D., Sady, N., Walter, C., et al., 2006. Relationships between particle-size distribution and organic carbon in French arable topsoils. Soil Use Manage. 22, 48–51.
Bao, Y.F., Ding, G.D., Wu, B., et al., 2013. Study on the wind-sand flow structure of windward slope in the Mu Us Desert, China. J. Food Agric. Environ. 11 (2), 1449–1454.
Basso, B., De Simone, L., Cammarano, D., et al., 2012. Evaluating responses to land degradation mitigation measures in Southern Italy. Int. J. Environ. Res. 6, 367–380.
Carter, M.R., Angers, D.A., Gregorich, E.G., et al., 2003. Characterizing organic matter retention for surface soils in Eastern Canada using density and particle size fractions. Can. J. Soil Sci. 83, 11–23.
Cao, S.X., 2008. Why large-scale afforestation efforts in China have failed to solve the desertification problem. Environ. Sci. Technol. 42, 1826–1831.
Cao, S.X., Chen, L., Shankman, D., et al., 2011. Excessive reliance on afforestation in China's arid and semi-arid regions: Lesson in ecological restoration. Earth-Sci. Rev. 104, 240–245.
Chen, X.H., Duan, Z.H., 2009. Changes in soil physical and chemical properties during reversal of desertification in Yanchi County of Ningxia Hui autonomous region, China. Environ. Geol. 57, 975–985.
Chen, Y., Tang, H., 2005. Desertification in north China: background, anthropogenic impacts and failures in combating it. Land Degrad. Dev. 16, 367–376.
Duan, Z.H., Xiao, H.L., Li, X.R., et al., 2004. Evolution of soil properties on stabilized sands in the Tengger Desert, China. Geomorphology 59, 237–246.
Falconer, K., 2003. Fractal Geometry: Mathematical Foundations and Applications, 2nd ed. Chichester, Wiley, England.
Gao, G.L., Ding, G.D., Wu, B., et al., 2014. Fractal scaling of particle size distribution and relationships with topsoil properties affected by biological soil crusts. Plos ONE 9, e88559.
Gui, D.W., Lei, J.Q., Zeng, F.J., et al., 2010. Characterizing variations in soil particle size distribution in oasis farmlands – a case study of the Cele Oasis. Math. Comput. Model. 51, 1306–1311.
Huang, C.Y., 2010. Soil Science, 3rd ed. China Agriculture Press, Beijing (in Chinese).
Jiao, F., Wen, Z.M., Shao, M.A., 2011. Changes in soil properties across a chronosequence of vegetation restoration on the Loess Plateau of China. Catena 86, 110–116.
Jin, Z., Dong, Y.S., Qi, Y.C., et al., 2013. Characterizing variations in soil particle-size distribution along a grass-desert shrub transition in the Ordos Plateau of Inner Mongolia, China. Land Degrad. Dev. 24, 141–146.
Institute of Soil Science, Chinese Academy of Sciences, 1978. Soil Physical and Chemical Analysis. Shanghai Science Technology Press, Shanghai (in Chinese).
Li, W.H., 2004. Degradation and restoration of forest ecosystems in China. Forest Ecol. Manag. 201, 33–41.
Li, X.R., He, M.Z., Duan, Z.H., et al., 2007. Recovery of topsoil physicochemical properties in revegetated sites in the sand-burial ecosystems of the Tengger Desert, northern China. Geomorphology 88, 254–265.
Li, X.R., Xiao, H.L., He, M.Z., et al., 2006. Sand barriers of straw checkerboards for habitat restoration in extremely arid desert regions. Ecol. Eng. 28, 149–157.
Li, X.R., Zhang, Z.S., Zhang, J.G., et al., 2004. Association between vegetation patterns and soil properties in the Southeastern Tengger Desert, China. Arid Land Res. Manag. 18, 369–383.
Li, X.R., Zhao, Y.X., Yang, Z.Z., et al., 1999. Study on evolution of air seeding vegetation and habitat in Maowusu Sandland. Acta Phytoecol. Sin. 23, 116–124 (in Chinese).
Normile, D., 2007. Getting at the roots of killer dust storms. Science 317, 314–316.
Otani, S., Onishi, K., Mu, H., et al., 2012. The relationship between skin symptoms and allergic reactions to Asian dust. Int. J. Environ. Res. Pub. Health 9, 4606–4614.
Qi, Y., Wang, Y.M., Wang, J.H., et al., 2003. Analysis on desertification dynamics based on remote sensing and GIS-exampled in Yanchi County, Ningxia. J. Desert Res. 23, 275–279 (in Chinese).
Rumpel, C., Eusterhues, K., Kogel-Knabner, I., 2004. Location and chemical composition of stabilized organic carbon in topsoil and subsoil horizon of two acid forest soils. Soil Biol. Biochem. 36, 177–190.
Su, Y.Z., Zhang, T.H., Li, Y.L., et al., 2005. Changes in soil properties after establishment of *Artemisia halodendron* and *Caragana microphylla* on shifting sand dunes in semiarid Horqin Sandy Land, Northern China. Environ. Manag. 36, 272–281.
Su, Y.Z., Zhao, H.L., Zhao, W.Z., et al., 2004. Fractal features of soil particle size distribution and the implication for indicating desertification. Groderma 122, 43–49.
Tavili, A., Jafari, M., 2009. Interrelations between plants and environmental variables. Int. J. Environ. Res. 3, 239–246.
Tyler, S.W., Wheatcraft, S.W., 1990. Fractal processes in soil water retention. Water Resour. Res. 26, 1047–1054.
Wang, G.L., Zhou, S.L., Zhao, Q.G., 2005. Fractal dimension of soil particle volume distribution and its application in land use. Acta Pedol. Sin. 42, 545–550 (in Chinese).
Wang, X.D., Li, M.H., Liu, S.Z., et al., 2006. Fractal characteristics of soils under different land use patterns in the arid and semiarid regions of the Tibetan Plateau, China. Geoderma 134, 56–61.
Wang, X.M., Chen, F.H., Hasi, E., et al., 2008. Desertification in China: an assessment. Earth-Sci. Rev. 88, 188–206.
Wang, X.M., Zhang, C.X., Hasi, E., et al., 2010. Has the Three Norths Forest Shelterbelt Program solved the desertification and dust storm problems in arid and semiarid China? J. Arid Environ. 74, 13–22.

Xu, D.H., Fang, X.W., Su, P.X., et al., 2012. Ecophysiological responses of *Caragana korshinskii* Kom. under extreme drought stress: leaf abscission and stem survives. Photosynthetica 50, 541–548.

Yang, W.B., Ding, G.D., Wang, J.Y., et al., 2006. Windbreak effects of belt scheme *Caragana korshinskili* Kom. plantation for sand-fixation. Acta Ecol. Sin. 26, 4106–4112 (in Chinese).

Yang, W.X., 1996. The preliminary discussion on soil desiccation of artificial vegetation in the northern regions of China. Sci. Silvae Sin. 32, 78–85 (in Chinese).

Zha, Y., Gao, J., 1997. Characteristics of desertification and its rehabilitation in China. J. Arid Environ. 37, 419–432.